VU VRIJE UNIVERSITEIT AMSTERDAM

VU Research Portal

Surface coating and particle size are main factors explaining the transcriptome-wide responses of the earthworm Lumbricus rubellus to silver nanoparticles

Roelofs, Dick; Makama, Sunday; De Boer, Tjalf E.; Vooijs, Riet; Van Gestel, Cornelis A.M.; Van Den Brink, Nico W.

published in
Environmental Science. Nano
2020

DOI (link to publisher)
10.1039/c9en01144g

document version
Publisher's PDF, also known as Version of record

document license
Article 25fa Dutch Copyright Act

Link to publication in VU Research Portal

citation for published version (APA)
Roelofs, D., Makama, S., De Boer, T. E., Vooijs, R., Van Gestel, C. A. M., & Van Den Brink, N. W. (2020). Surface coating and particle size are main factors explaining the transcriptome-wide responses of the earthworm Lumbricus rubellus to silver nanoparticles. *Environmental Science. Nano*, *7*(4), 1179-1193. https://doi.org/10.1039/c9en01144g

General rights
Copyright and moral rights for the publications made accessible in the public portal are retained by the authors and/or other copyright owners and it is a condition of accessing publications that users recognise and abide by the legal requirements associated with these rights.

- Users may download and print one copy of any publication from the public portal for the purpose of private study or research.
- You may not further distribute the material or use it for any profit-making activity or commercial gain
- You may freely distribute the URL identifying the publication in the public portal ?

Take down policy
If you believe that this document breaches copyright please contact us providing details, and we will remove access to the work immediately and investigate your claim.

E-mail address:
vuresearchportal.ub@vu.nl

Download date: 27. May. 2021

Environmental Science Nano

ROYAL SOCIETY OF CHEMISTRY

PAPER

View Article Online
View Journal | View Issue

Published on 19 February 2020. Downloaded by VRIJE UNIVERSITEIT on 3/1/2021 2:08:35 PM.

Check for updates

Cite this: *Environ. Sci.: Nano*, 2020, 7, 1179

Surface coating and particle size are main factors explaining the transcriptome-wide responses of the earthworm *Lumbricus rubellus* to silver nanoparticles†

Dick Roelofs, ‡*[a] Sunday Makama, ‡[b] Tjalf E. de Boer,[c] Riet Vooijs,[a] Cornelis A. M. van Gestel[a] and Nico W. van den Brink[b]

Received 8th October 2019,
Accepted 18th February 2020

DOI: 10.1039/c9en01144g

rsc.li/es-nano

Due to the unique properties of differently sized and coated silver nanoparticles (AgNPs), they are used in important industrial and biomedical applications. However, their environmental fate in soil ecosystems and potential mechanisms of toxicity remain elusive, especially at the level of transcriptional regulation. We investigated the transcriptome-wide responses of the earthworm *Lumbricus rubellus* exposed to nine AgNPs differing in surface coating/charge (bovine serum albumin/negative AgNP_BSA, chitosan/positive AgNP_Chit, and polyvinylpyrrolidone/neutral AgNP_PVP) and sizes (20, 35 and 50 nm) at concentrations close to the EC_{50} value related to reproduction. $AgNO_3$ was used in two concentrations to benchmark the AgNP effects against those of the Ag salt. A correlation was observed between the number of differentially expressed genes (DEGs) and Ag internal body concentration. Only metallothionein was regulated by all treatments. Medium sized AgNPs caused the most pronounced transcriptional responses, while $AgNO_3$ affected the transcriptome less. Medium sized AgNP_BSA exposure caused the most extensive transcriptional responses with 684 DEGs. Gene ontology enrichment analysis of medium sized AgNP_BSA affected DEGs revealed that mitochondrial electron transport, autophagy and phagocytosis, mesoderm and heart development and microtubule organisation were affected. This was also confirmed by gene set enrichment for KEGG pathway analysis, indicating that phagocytosis, autophagy and signalling pathways related to mesoderm formation were significantly up regulated. All AgNP_BSA and AgNP_PVP exposures caused severe down regulation of ribosomal translation, suggesting that the high energy-demanding protein synthesis process is inhibited. Our data confirm the mechanisms previously identified among other animal models and human cell lines. To conclude, coating formulation and particle size severely impact transcriptional responses at a particular nanoparticle size, suggesting diverse mechanistic responses depending on the coating type.

Environmental significance

Nanoparticles enter the environment in different sizes and with different coatings, potentially leading to form and coating specific effects on organisms. Risk assessment of nanomaterials should take this into account and benefits from possibilities of read-across between similar forms of nanomaterials and also between species. We assessed the transcriptomic responses of the earthworm *Lumbricus rubellus* to silver nanoparticles (AgNPs) of varying sizes and coatings. Responses were dependent on the particle size and coating type; medium-sized BSA coated AgNPs exerted the most pronounced transcriptomic responses. To conceptualize these mechanistic responses, we linked differential gene expression to physiological pathways. We confirmed the molecular mechanisms of AgNP toxicity suggested in previous studies using different models, opening the way to extrapolate AgNP effects on different organisms.

Introduction

The nanotechnology industry continues to grow, with silver nanoparticles (AgNPs) being recognised as the most commonly used nanomaterial in many applications, owing to their excellent antimicrobial activity and superior physicochemical characteristics.[1,2] The global market demands for AgNPs have been projected to reach $2.5 billion

[a] *Department of Ecological Science, Faculty of Science, Vrije Universiteit, Amsterdam, De Boelelaan 1085, 1081 HV Amsterdam, The Netherlands. E-mail: dick.roelofs@gmail.com; Fax: +31 20 5987123; Tel: +31 20 5987078*
[b] *Department of Toxicology, Wageningen University, Wageningen, The Netherlands*
[c] *MicroLife Solutions, Amsterdam, The Netherlands*

† Electronic supplementary information (ESI) available. See DOI: 10.1039/c9en01144g

‡ These authors contributed equally to this work.

Published on 19 February 2020. Downloaded by VRIJE UNIVERSITEIT on 3/1/2021 2:08:35 PM.

by the year 2022.[3] This raises environmental health concerns over the likelihood of their release into the environment, a potential outcome supported by a 130 times increase (from 0.1 μg kg^{-1} to 13 μg kg^{-1}) in the predicted soil concentrations of AgNPs in the United States[4–7] in 2009. In recent years, therefore, AgNPs have been increasingly investigated.[2,8] Nevertheless, environmental effects of AgNPs are still not well understood and information on the effects of particle size and coating type on biota are limited.

Generally, the available literature has revealed possible mechanisms that may be involved in the toxicity of AgNPs. Common among these is oxidative stress due to increased generation of reactive oxygen species (ROS), or failure of the organism's protective mechanisms against these radicals. An increase in ROS production has been reported both *in vitro* and *in vivo* in mammalian cells,[9,10] bacteria,[11] rodents[12] and earthworms[13] exposed to AgNPs. Also, the role of silver ions (Ag^+) released from AgNPs in mediating toxic effects has been described.[14] This does not exclude the involvement of AgNPs directly, as several studies showed that the toxicity was caused by the NPs.[13,14] Also, evidence is available for the uptake of particulate Ag in earthworms[15,16] and mice/rats[17] exposed to AgNPs.

Recently, investigations utilizing both *in vivo* and *in vitro* models[18,19] have enhanced our knowledge on the fate and effects of various NPs following different exposure scenarios. These studies point at a number of physicochemical properties including size, shape, surface chemistry (charge), and agglomeration and dissolution rates,[20,21] playing significant roles in influencing the accumulation and toxicity of the tested NPs. The importance of the different properties in driving these processes, however, was not consistent and often varied between studies.[19] Some studies have reported clear effects of size,[22] while charge was more important in others.[23,24] Other investigators found no effect of NP size nor charge, but rather pointed at the roles of dissolved silver ions and surface coating, not related to the charge of the NPs.[21,25] Considering these conflicting results, a better understanding of the influence of the physicochemical properties of AgNPs on their fate and effects on organisms will facilitate a proper assessment of their potential risk.

Transcriptomic analysis of microarray or RNA sequencing (RNAseq) data is a powerful technology to investigate gene networks that are differentially regulated in response to toxicants at any given time.[26,27] For instance, Poynton *et al.*[28] used microarray analysis to investigate differences in the response of daphnids to AgNPs that were either citrate- or PVP coated. When the different coatings were related to $AgNO_3$ exposures, very distinct transcriptional profiles were revealed between particulate and ionic Ag. This suggests that AgNP induced toxicity profiles were mechanistically different from ionic Ag toxicity profiles. Main processes affected by AgNPs were protein metabolism and signal transduction, while $AgNO_3$ caused down-regulation of developmental processes and more specifically of sensory development.[28] In the nematode *Caenorhabditis elegans*, toxicogenomic investigation of AgNP toxicity revealed a clear signature of oxidative stress and activation of proteins involved in dauer larvae formation that could directly be linked to reproductive failure.[29] Such studies indicate that investigations on gene expression profiles may provide a more comprehensive mechanistic understanding of toxicological effects caused by nanoparticles. Also, it may be possible to distinguish these effects from the ones caused by metal ion exposures. The effects of PVP-coated AgNPs and $AgNO_3$ on the differential gene expression (microarray) response of *Enchytraeus albidus* following exposure in soil revealed higher toxicity when exposed to $AgNO_3$.[4] It was indicated that the responses observed due to exposure to AgNPs reflected an effect of Ag^+ ions, given the extent of similar or dissimilar genes activated. Genes related to developmental processes were activated in response to both treatments, while only the $AgNO_3$-treated groups showed activation of genes related to reproduction and cellular and metabolic processes.

In the current study, we tested the hypothesis that both the size and surface coating (charge) of AgNPs affect the gene expression profile of an exposed model terrestrial invertebrate. Exposures were performed using specifically synthesized AgNPs that differed in size and surface chemistry (charge). The red earthworm *L. rubellus* was used, representing an ecologically relevant species that is a very common upper soil-dwelling detritivore in most parts of Europe. Being an abundant species in soil, *L. rubellus* could serve as an indicator for the risks of soil contaminants. It has commonly been used in ecotoxicological studies on NPs[30,31] and other contaminants like zinc, lead and polycyclic hydrocarbons.[32] Here, we extend the approach described by Poynton *et al.*[28] and included three different coating types of AgNPs, also varying in mean core size. RNAseq techniques were used to monitor the profiles of gene expression occurring in the earthworms exposed to different forms of AgNPs at concentrations corresponding to the EC_{50} values for effects on cocoon production.[33] Ionic Ag ($AgNO_3$) exposures were also included at the level of EC_{50} for cocoon production. The outcome of this study will provide insight into the gene expression profiles of a model terrestrial invertebrate as a result of AgNP exposure under environmentally relevant conditions, and how the AgNP properties may influence these. Subtle (mild) effects, not easily detectable by other toxicological endpoints, may be identified based on gene ontology, shedding light on the likely mechanisms of toxicity involved in the outcomes observed at the population level determined in earlier studies.[33]

Methods

Synthesis and characterisation of AgNPs

AgNPs used in this study were synthesized at the Catalonia Institute of Nanoscience and Nanotechnology (Institut Català de Nanociència i Nanotecnologia (ICN2)), Barcelona, Spain. Details of the synthesis and characterisation of the AgNPs have been reported previously[33] and are only briefly discussed here. Colloidal, dispersed AgNPs of three different

 This journal is © The Royal Society of Chemistry 2020

Published on 19 February 2020. Downloaded by VRIJE UNIVERSITEIT on 3/1/2021 2:08:35 PM.

sizes (20, 35 and 50 nm) were prepared separately, following a kinetically controlled seeded-growth method[34] with slight modifications. This approach is based on the reduction of silver nitrate ($AgNO_3$) in the presence of two competing reducing agents, tannic acid (TA) and trisodium citrate hexahydrate (SC) at 100 °C. The resulting AgNPs were surface-coated with bovine serum albumin (BSA), chitosan (Chit) or polyvinylpyrrolidone (PVP) to generate negatively charged AgNP_BSA, positively charged AgNP_Chit and neutral AgNP_PVP, respectively. The three sizes investigated were chosen based on literature reports which suggested nanotoxicity in the 20–50 nm range.[33]

All nine AgNPs were dispersed in soil extracts and MilliQ water and characterised by a combination of different techniques.[24,33] Particle size distributions were assessed by single-particle inductively coupled plasma-mass spectrometry (spICP-MS), while core mean sizes were determined by transmission electron microscopy (TEM). UV-vis, dynamic light scattering (DLS), and zeta-potential measurements (ζ-potential) were used to monitor the stability of the AgNPs in different media and to determine their surface charges. Results of characterisation are discussed only briefly here, and the reader is referred to our earlier work for more details.[24,33]

Soil preparation and earthworm exposure experiment

Soil preparation and spiking using soil extract were performed according to the study of van der Ploeg *et al.*[35] Briefly, sifted air-dried natural soil with pH_{KCl} 5.1 and 3.8% organic matter obtained from a reference experimental organic farm (Proefboerderij Kooijenburg, Marwijksoord, The Netherlands) was used for the experiment. Soil extract made from the same soil was used to prepare AgNP suspensions and solutions of $AgNO_3$ as previously reported.[16] Earthworms were exposed for 72 h to AgNPs with nominal exposure concentrations of 0, 15.63, 31.25, 62.5, 125 and 250 mg Ag per kg dry soil. The exposure duration of 72 h was based on the literature which indicated that most effects at the level of gene expression were significant following 3 day exposures.[36,37] To compare the effects of ionic silver (Ag^+), two $AgNO_3$ concentrations were also included (1.5 and 15 mg Ag per kg dry soil). The two concentrations were selected because of uncertainty in the potential dissolution of the AgNPs, depending on their coating.[38] To avoid potential differences in uptake between the different treatments, all dose–response relationships will be based on the actual uptake of Ag, as expressed by the internal concentrations in the earthworms. Control earthworms were kept in clean soil without added AgNPs or $AgNO_3$. At the end of the exposure period, earthworms were collected and analysed for total Ag bioaccumulation and for gene expression profiles. The $AgNO_3$ concentrations were selected to benchmark the AgNP sublethal effects against those of the Ag salt.[15,33] van der Ploeg *et al.* also showed that 1 and 15 mg kg^{-1} correspond to the NOEC and a 50% decrease in the relative survival of earthworm coelomocytes.[15] Furthermore, exposure experiments differed in time, in that each exposure with a particular coating type was performed at a different time point with a particular batch of animals. To control for these temporal differences, we included independent ion exposures and controls for each coating type. The control soil was treated with only soil extract and deionised water (Millipore; resistivity = 18.2 MΩ cm^{-1}). Soil spiking and/or moistening was conducted 24 h before introducing the earthworms during which the moistened soil was allowed to equilibrate under climate-controlled conditions of 24 h light cycle, 15 °C, and 61% relative humidity. The moisture content of the soil was re-adjusted to attain 50% of its water holding capacity.

Clitellated adult earthworms (*L. rubellus*) having no gross lesions and of 1–2.5 g live weight were obtained from an uncontaminated site in The Netherlands (Nijkerkerveen). They were acclimatized in uncontaminated soil for two weeks under the same conditions as described above, weighed and distributed randomly in experimental units (jars). Each treatment was prepared in triplicate at a density of 5 animals per jar.

Sample collection and preparation

At the end of the 72 h exposure period, surviving earthworms were collected from each replicate. These were weighed, placed into glass Petri-dishes lined with moistened Whatman® filter paper no. 597 (Fisher Scientific, Pittsburg, PA) and allowed to depurate over 48 h.[16] The earthworms were kept at the same temperature as that during the exposure period. Following gut-emptying, the earthworms were washed with demineralized water, pad-dried with absorbent paper and snap frozen in liquid nitrogen. Samples were preserved at −80 °C until analysis. One earthworm from each replicate was used for gene expression analysis, while before quantification of the total Ag concentration, whole earthworm tissues were ground to powder in liquid nitrogen using a mortar and pestle, pooling two individuals per experimental unit.

Quantification of Ag in earthworm tissues

To quantify the total Ag tissue concentrations in earthworm samples, 250 mg of the crushed tissue from each replicate was weighed in digestion tubes and 1.0 mL of MilliQ water, 0.5 mL of 65% HNO_3 and 1.5 mL of 37% HCl were added and mixed gently by swirling the capped tubes. The tubes were then incubated for 30 min in a water bath at 60 °C. After cooling down to room temperature, the resulting digest was diluted and the total Ag content measured by inductively-coupled plasma mass spectrometry (ICP-MS). The analysis was conducted using a Thermo X Series 2 ICP-MS equipped with an auto-sampler and a conical glass concentric nebuliser and operated at a radio frequency power of 1400 W. Data acquisition was performed in the selected ion mode at the m/z ratio of 107 characteristic for silver. Quantification was based on ionic silver standards diluted in the same

Published on 19 February 2020. Downloaded by VRIJE UNIVERSITEIT on 3/1/2021 2:08:35 PM.

acidic matrix. The detection limit for the total tissue Ag concentration using the described procedure for ICP-MS was about 50 ng per kg tissue DW.

Uptake data obtained for the 72 hour exposure were processed using Microsoft Excel (2016), and subsequently subjected to one-way analysis of variance (ANOVA) with the aid of GraphPad Prism 8.02 for Windows (GraphPad Software, San Diego California USA, www.graphpad.com). All results are presented as mean ± standard deviation (s.d.), and a p value of <0.05 is considered to be significant.

RNA isolation and normalization

All controls and treatments of exposed worms were conducted in triplicate. The earthworms selected for RNAseq were sampled from experimental units treated at AgNP exposure concentrations closest and within the standard error limits of the EC_{50} values as confirmed by Makama *et al.*[33] (Table 1) for effects on earthworm reproduction (no. of cocoons laid), which was the most sensitive toxicity endpoint in a 28 day sub-chronic study using the same AgNPs.[33]

For each coating type we analysed the gene expression of earthworms exposed to small, medium and large sized AgNPs. To control for temporal and animal batch differences, two ionic $AgNO_3$ exposures (1.5 and 15 mg Ag^+ kg^{-1}) and a control (natural soil only) were used for each coating type. In total, 54 samples were prepared for RNA extraction and subsequent sequencing. Each earthworm (representing a single replicate) was crushed in liquid nitrogen and a sub-sample of 25 mg was taken for total RNA extraction using an SV total RNA isolation system according to the manufacturer's instructions (Promega, US). Slight modifications included addition of 500 μl dilution buffer, 285 μl ethanol and 800 μl wash buffer. Total RNA was quantified using a NanoDrop ND-1000 UV-vis spectrometer (Thermo Fisher Scientific). About 1 μg of total RNA was subjected to cDNA synthesis using a TruSeq RNA sample preparation kit v2 according to the manufacturer's instructions (Illumina, US). Subsequently, samples were quality checked and quantified by running them on a BioAnalyzer lab-on-a-chip (Agilent, US).

Table 1 EC_{50} exposure concentrations applied for RNAseq analysis based on cocoon production.[33] Xs depict chosen concentrations for each AgNP coating type and size that were close to EC_{50} (cocoon production) and within the EC_{50} confidence limits. Nominal AgNP concentrations are in mg per kg dry soil

	Charge	Negative	Positive	Neutral
NP size	[mg kg^{-1}]	BSA	CHITOSAN	PVP55
Small	62.5	X		X
20 nm	250		X	
Medium	62.5			X
35 nm	125	X		
	250		X	
Large	62.5	X		
50 nm	250		X	X
$AgNO_3$	1.5	X	X	X
	15	X	X	X
Control	0	X	X	X

RNA sequencing

The 54 samples were assigned a unique sequencing barcode and total RNA from each sample was prepared for Illumina HiSeq sequencing. Sequence libraries were prepared by adding equal amounts of each sample to the library pool. Paired-end 125 bp sequencing was performed on an Illumina HiSeq 2500 by dividing the samples over three lanes of a flow cell. After sequencing, the individual samples were demultiplexed by barcode.

Assembly and data analysis

FastQC was applied to quality control the raw sequence reads. Low quality bases were trimmed using Trimmomatic (quality cut-off of 24 using the Phred33 encoding).[39] The mapping references represented an assembled transcriptome previously generated and kindly provided by Prof. P. Kille (University of Cardiff), which we were able to re-assemble from approximately 160 000 to approximately 51 000 (51k) transcript sequences. This 51k transcriptome assembly was annotated using the pipeline incorporated in the Omics Box (previously called BLAST2GO) from BioBam bioinformatics solutions (https://www.biobam.com/omicsbox/). Gene ontology (GO) terms were predicted based on BlastP hits and InterPro domains against the non-redundant UniProt/TrEMBL database (*E*-value threshold of 1×10^{-5}). Mapping and read quantification was conducted using a combination of Bowtie2/SAMtools using default settings using a maximum fragment length of 800 bp, allowing 3 mismatches in the 'report all alignment' option. Counting of uniquely mapped reads was performed using eXpress.[40,41] Differential gene expression analysis was performed in R using the EdgeR package[42] which applies a general linear model by contrasting each particle size per coating type to the control conditions followed by a correction for multiple testing using the false discovery rate method.[43] This yielded five sets of significant (false discovery rate FDR corrected $p < 0.05$) genes per coating type (20, 35 and 50 nm AgNPs, and low and high ionic Ag^+) that were each subjected to gene ontology (GO) enrichment analysis using the TopGO package in R[44] (Fisher's exact test with FDR corrected $p < 0.1$). In total, 6438 GO terms were associated to annotated genes, which were taken as a reference list in the enrichment analysis. Enriched GO terms that only contained one transcript were removed from the significant GO term list and omitted from further analysis. Assembly and raw data associated with this present study are publicly available in NCBI under bioproject number PRJNA566139. Multi-dimensional scaling plots of significantly enriched GO terms were generated using the REVIGO interface.[45] REVIGO summarizes long GO lists by reducing functional redundancy in GO terms based on semantic similarity in ontology descriptions.[46] The main GO terms in the summarized list are subsequently plotted as

 This journal is © The Royal Society of Chemistry 2020

Published on 19 February 2020. Downloaded by VRIJE UNIVERSITEIT on 3/1/2021 2:08:35 PM.

colored circles in a two dimensional matrix, visualizing their relatedness using multidimensional scaling by eigenvalue decomposition again based on semantic similarity of the GO term description. Additional KEGG ortholog annotation was performed using the KEGG Automatic Annotation Server (http://www.genome.jp/tools/kaas/)[47] and gene expression pathway analysis was performed using the Generally Applicable Gene-set Enrichment for pathway analysis R-package GAGE combined with Pathview using standard settings.[48] GAGE identifies coordinated differential expression in gene sets among functionally related groups of genes belonging to a certain biological pathway pre-defined by KEGG. As input for the pathway analysis we used the gene expression fold change ratios as determined by differential expression in response to the different coated AgNPs. Pathways were considered significantly up- or down-regulated with a FDR-corrected p-value < 0.1. Coordinated up- or down-regulation of functionally related genes was visualised by plotting color coded up (red) and down (green) regulation on the pathway topology derived from KEGG.

Results

AgNP pre-exposure characterisation

The AgNPs used in this study have been fully characterised earlier, and detailed information on this can be found in ref. 24 and 33. Before coating the AgNPs with BSA, chitosan or PVP, the SPR peaks were centred at 405, 430 and 441 nm, while the hydrodynamic sizes for 20, 35 and 50 nm AgNPs were 36, 46 and 55 nm, respectively. Average particle sizes (nm) obtained by analysis of over 250 nanoparticles by TEM were 19.5 ± 5.4, 37.4 ± 3.7 and 51.1 ± 5.7 nm (AgNP_BSA);, 18.2 ± 5.1, 37.2 ± 4.3 and 51.9 ± 6.4 nm (AgNP_Chit), and 24.0 ± 4.6, 38.2 ± 4.5 and 51.0 ± 6.1 nm (AgNP_PVP) for the 20, 35 and 50 nm size groups, respectively (average ± s.d.). The shapes of the SPR peaks in both MilliQ water and soil extract were generally preserved except for those of the 20 nm AgNP_PVP and 35 and 50 nm AgNP_Chit suspensions in soil extract, whose SPR peaks suggested formation of some agglomerates. Dispersion in soil extract showed preserved ζ-potentials for AgNP_BSA and AgNP_Chit. All sizes of AgNP_PVP, however, presented negative ζ-potentials, but the values were less negative than those for AgNP_BSA.[24,33]

Ag uptake in earthworms

The negatively charged AgNP_BSA showed the highest uptake, in particular the 35 nm AgNP_BSA particles (Table 2), although this was not significantly different between three NP size ranges for the individual coating type. When considering the chitosan coating, the highest uptake was also observed during exposure to medium sized (53.8 ± 50.5 35 nm) particles, but due to a very high standard error this uptake was not significantly different from the Ag uptake observed with 20 nm and 50 nm AgNP_Chit. The Ag uptake of 50 nm AgNP_PVP seemed the highest among all AgNP_PVP exposures, but this was again not significant. The uptake of Ag from $AgNO_3$ was in the same order of magnitude as that from the AgNPs when comparing nominal exposure concentrations on a mass basis (Tables 1 and 2), providing a suitable benchmark for AgNP uptake.

Gene expression (RNAseq)

The 54 RNAseq library samples were randomly distributed over three pooled libraries. On average, 98.3% of both forward and reverse reads passed the set quality threshold and remained available for further analysis. The library sizes per sample were 1.10×10^6 reads on average with variation ranging from 0.85×10^6 to 1.37×10^6 reads. Reads were subsequently mapped to the reference transcriptome with an average mapping success rate of 69.4%. Natural variation among the earthworms caused the mapping rate to range from 50% to 80% randomly distributed among animal samples. Nevertheless, statistical analyses showed significantly regulated gene expression patterns.

Internal Ag concentration and differential gene expression

Table 2 gives a general overview of the total number of differentially expressed genes (DEGs) in adult *L. rubellus* upon 72 h exposure to the different AgNPs in natural soil at an exposure concentration around the EC_{50} values for their effects on reproduction (detailed gene lists with gene annotations are given in ESI† files 1–3). The medium sized (35 nm) NPs elicited high numbers of DEGs for all types of coating. Exposure to the 20 and 50 nm sized AgNPs was associated with lower numbers of DEGs with averages of 25 and 11, respectively (Table 2). Surface coating did not influence transcriptional regulation by the smaller sized- and larger sized AgNP exposures. Ionic Ag^+ had only a minor effect on gene expression at both concentrations

Table 2 Uptake of Ag from AgNPs and ionic Ag^+, and the number of significantly differentially regulated transcripts when compared to those from control animals (over 3 biological replicates) identified using RNAseq analysis in the earthworm *Lumbricus rubellus* exposed for 72 h to differently coated 20, 35 and 50 nm AgNPs in natural soil. AgNP_BSA (negative, bovine serum albumin-coated); AgNP_Chit (positive, chitosan-coated); AgNP_PVP (neutral, polyvinylpyrrolidone-coated)

		AgNP_BSA (negative)		AgNP_Chit (positive)		AgNP_PVP (neutral)	
		mg per kg tissue	# DEGs	mg per kg tissue	# DEGs	mg per kg tissue	# DEGs
Small (20 nm)		37.8 ± 14.2	29	47.5 ± 31.4	23	33.4 ± 8.6	24
Medium (35 nm)		74.9 ± 28.7	684	53.8 ± 50.5	246	26.6 ± 17.2	80
Large (50 nm)		26.0 ± 6.7	11	35.9 ± 27.5	12	50.7 ± 27.3	9
$AgNO_3$	Low (L)	3.1 ± 0.5	4	2.2 ± 0.9	12	1.7 ± 0.3	1
	High (H)	38.3 ± 26.2	29	26.1 ± 9.7	31	22.2 ± 14.8	16

Published on 19 February 2020. Downloaded by VRIJE UNIVERSITEIT on 3/1/2021 2:08:35 PM.

tested, with affected numbers of DEGs being similar to those of the 20 and 50 nm AgNPs (Table 2). All lists of DEGs associated with each of the different exposure types are provided in ESI† files 1–3 for AgNP_BSA, AgNP_Chit and AgNP_PVP, respectively.

As mentioned above, exposure to the medium-sized AgNPs caused the most pronounced responses at the transcriptional level, accounting for over 90% of the differentially regulated transcripts. Among the different coating types, AgNP_BSA induced the most extensive transcriptional responses: 684 genes (95%) were up- or down-regulated upon exposure to the 35 nm AgNP_BSA (Table 2). A significant correlation between the internal tissue Ag concentration and the number of DEGs was observed among all coated AgNPs (Pearson's correlation $r = 0.84$, $p = 0.007$, Fig. 1). This correlation was the most pronounced among medium-sized AgNPs, where the AgNP_PVP coated particles showed the lowest number of affected transcripts and internal Ag, while that of internal Ag and affected transcripts by medium-sized AgNP_BSA exposure was the highest.

Fig. 2a presents the Venn diagram of all DEGs affected by exposure to 35 nm AgNPs for all three coating types. Metallothionein (MT) was the only DEG present in all treatments. Medium-sized AgNP_BSA and AgNP_Chit exposures showed the most overlap with 61 co-regulated genes. In contrast, medium-sized AgNP_PVP showed hardly any commonality in transcriptional regulation when compared to the other two medium-sized coated AgNPs.

Gene expression and particle size

Comparing gene expression responses elicited by AgNPs with different sizes for each coating type hardly revealed any

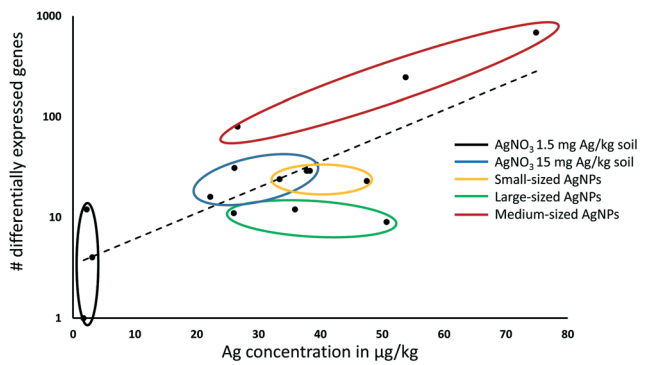

Fig. 1 Relationship between the numbers of significant differentially expressed genes (DEGs) and the tissue Ag concentrations in the earthworms *Lumbricus rubellus* exposed for 72 h to 20, 35 and 50 nm AgNPs with different surface coatings: AgNP_BSA (negative, bovine serum albumin-coated); AgNP_Chit (positive, chitosan-coated); AgNP_PVP (neutral, polyvinylpyrrolidone-coated). DEGs produced by $AgNO_3$ low (1.5 mg Ag per kg dry soil) and high (15 mg Ag per kg dry soil) exposures are also included. Circles represent different types of treatments: black, $AgNO_3$ 1.5 mg Ag per kg dry soil; blue, $AgNO_3$ 15 mg per kg dry soil; yellow, small-sized AgNPs; green, large-sized AgNPs; red, medium-sized AgNPs. *X*-Axis, Ag concentration in mg per kg tissue; *y*-axis, log10 DEG counts. Dashed line represents the exponential trend line.

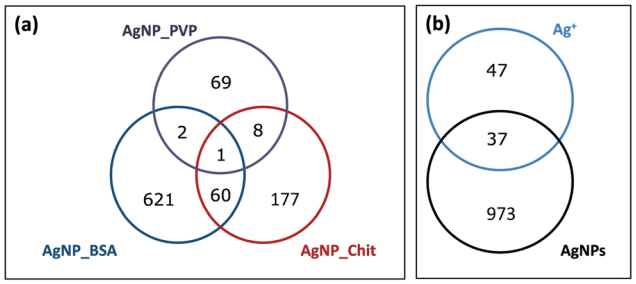

Fig. 2 Venn diagrams of significant differentially expressed genes (DEGs) in the earthworm *Lumbricus rubellus* after 72 h exposure to AgNPs and both ionic Ag ($AgNO_3$) treatments showing the overlap of significant DEGs responding to the treatments with all three coating types of 35 nm sized AgNPs (left panel, a), and between all combined DEGs responding to 35 nm-sized AgNPs and ionic Ag^+ (1.5 and 15 mg Ag per kg dry soil, right panel, b). AgNP_BSA (negative, bovine serum albumin-coated); AgNP_Chit (positive, chitosan-coated); AgNP_PVP (neutral, polyvinylpyrrolidone-coated).

overlap. More specifically, only 4 genes were differentially regulated among all sizes of AgNP_BSA, while among all AgNP_Chit NPs only 3 DEGs were identified. We found no overlap in differential expression among the different sizes of AgNP_PVP (ESI† file 3).

A total of 37 genes were shared among all DEGs responding to all medium-sized AgNP types (combined) and to ionic Ag treatments (Fig. 2b). The specific transcriptional profiles of these genes were analyzed in more detail and most of them (31 DEGs) showed highly similar responses, when comparing ionic Ag exposures to AgNP exposures: a subset of 27 were coordinately up-regulated, while 4 were coordinately down-regulated. However, 6 transcripts showed opposite regulation; they were up-regulated due to ionic Ag, but down-regulated in response to AgNP exposure. Among the annotated gene list of shared up-regulated genes we identified metallothionein, chitinase-3, caspase 7, ankyrin, midline-1 and cystathionine beta synthase. Unfortunately, no gene annotation was retrieved from a down-regulated transcript. Cubilin, a gene involved in endocytosis and earlier identified to be involved in AgNP toxicity[49] in earthworms, was identified among the dissimilarly regulated transcripts.

Gene ontology and gene set enrichment for pathways

The number of DEGs identified in the medium sized AgNP exposures allowed enrichment analysis by applying Fisher's exact test on all gene ontology (GO) categories represented by each set of DEGs to identify enriched biological processes and molecular functions. This GO enrichment analysis yielded 37 significantly enriched GO terms for AgNP_BSA, 17 for AgNP_Chit and 25 in case of AgNP_PVP exposure (ESI† file 4). Several biological processes were affected, related to development (mesoderm formation), oxidative phosphorylation, and autophagy.

When comparing enriched GO terms among different coating types, we observed no commonly affected processes.

This journal is © The Royal Society of Chemistry 2020

Published on 19 February 2020. Downloaded by VRIJE UNIVERSITEIT on 3/1/2021 2:08:35 PM.

However, all three coating types seemed to affect developmental processes, but in different ways. While BSA coated AgNP exposure affected mesoderm formation (Fig. 3), respiratory tube development was associated with AgNP_Chit exposure, and AgNP_PVP exposure affected regeneration. The main processes observed among significant GO terms associated with AgNP_Chit are related to cysteine and serine metabolism, while extracellular matrix organization and response to fibrinolysis are associated with AgNP_PVP (ESI† file 4).

Another way to retrieve functional mechanistic information from differentially regulated gene clusters is to subject them to pathway analysis. Generally Applicable Gene-set Enrichment for pathway analysis (GAGE) provides information on gene clusters in pathways that are either significantly up- or down-regulated. A full list of all significantly coordinately regulated KEGG pathways is provided in ESI† file 5. Table 3 shows the pathways that were significantly identified in three or more AgNP exposures.

Strikingly, ribosomal translation is mostly identified and severely down-regulated in all AgNP treatments, except for AgNP_Chit exposure where this pathway was up-regulated. As an example, consider Fig. 4 showing all protein-coding genes (boxes) functionally related to the ribosome, where as much as 46 proteins participating in protein synthesis are down-regulated in response to medium-sized AgNP_BSA exposure. Furthermore, several signalling pathways were also highly affected by AgNPs. Among them, we identified MAPK signalling (Fig. 5), Ras signalling and focal adhesion-related signalling as the most frequently affected pathways. These were significantly up-regulated among all AgNP_BSA treatments, while all these pathways were down-regulated by small- and large-sized AgNP_Chit exposures. In the case of MAPK signalling, Fig. 5 shows that 32 protein-coding genes functionally related to MAPK signalling are up-regulated in response to medium-sized AgNP_BSA, while AgNP_Chit exposure caused 37 genes in the MAPK signalling pathway to be down-regulated (ESI† file 5).

AgNP_BSA exposures exerted the most pronounced pathway responses among the three coating types. Interestingly, in all AgNP_BSA exposures, five pathways were significantly up-regulated, while four pathways were significantly down-regulated, regardless of particle size (Table 4). Four of the six up-regulated pathways are associated with cell signalling, and can be linked to developmental processes identified in the GO enrichment analysis (mesoderm formation, Fig. 5). As mentioned earlier, the down-regulated pathways are linked to general metabolism, such as ribosome, peroxisome, and fatty acid metabolism (Table 4).

Medium- and large-sized AgNP_BSA particles shared as much as 10 pathways that were regulated in a similar direction. Autophagy and serine/threonine kinase mammalian target of rapamycin (mTOR) signalling are interesting to mention, since many studies show that metal nanoparticles induced autophagy

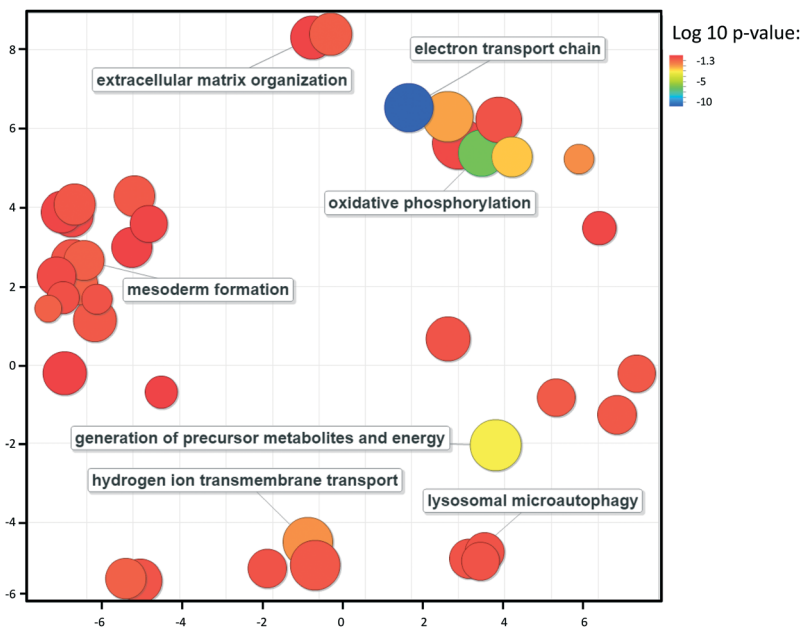

Fig. 3 Multidimensional scatter plot from REVIGO for significantly affected gene ontology (GO) terms of regulated genes in the earthworm *Lumbricus rubellus* upon 72 h exposure to medium-sized BSA-coated AgNPs in natural soil. The input GO terms were generated by GO enrichment analysis by using the TopGO package in R. Each circle represents a GO term and the circle size indicates the frequency of the GO term associated with significantly regulated DEGs. Biologically more related GO terms are clustered, and each cluster is named by its representative GO term. The color of the circles represents log10 *p*-values from the GO enrichment analysis, where red represents less significant GO terms and blue highly significant GO terms (Table S1†). *X*- and *y*-axes represent eigenvalues generated by multidimensional scaling of semantic relatedness of the GO terms in a pairwise distance matrix; more semantically similar GO terms are more related in the gene ontology structure and thus biologically more related.[45]

Published on 19 February 2020. Downloaded by VRIJE UNIVERSITEIT on 3/1/2021 2:08:35 PM.

Table 3 Significantly regulated pathways ($p < 0.05$) in *Lumbricus rubellus* affected by at least 3 Ag_NP exposure treatments. Column Up: the number of treatments the pathway was up-regulated; Down: the number of treatments the pathway was down-regulated. Treatment indicates which exposure exerted significant regulation of the particular pathway. BSA, AgNP_BSA exposure; Chit, AgNP_Chit exposure; PVP, AgNP_PVP exposure. The ko numbers represent the KEGG pathway codes

Affected pathways	Count			
Response	Up	Down	Total	Treatment
ko03010 ribosome	2	5	7	BSA/Chit/PVP
ko04010 MAPK signaling pathway	5	1	6	BSA/Chit
ko04014 Ras signaling pathway	3	2	5	BSA/Chit
ko04510 focal adhesion	3	2	5	BSA/Chit
ko04810 regulation of actin cytoskeleton	3	2	5	BSA/Chit
ko01120 microbial metabolism in diverse environments	1	3	4	BSA/PVP
ko01212 fatty acid metabolism	0	4	4	BSA/Chit
ko04012 ErbB signaling pathway	3	1	4	BSA/Chit
ko04015 Rap1 signaling pathway	2	2	4	BSA/Chit
ko04062 chemokine signaling pathway	2	2	4	BSA/Chit
ko04070 phosphatidylinositol signaling system	2	2	4	BSA/Chit
ko04722 neurotrophin signaling pathway	3	1	4	BSA/Chit
ko02010 ABC transporters	0	3	3	Chit
ko04020 calcium signaling pathway	1	2	3	BSA/Chit
ko04144 endocytosis	1	2	3	BSA/Chit
ko04146 peroxisome	0	3	3	BSA
ko04912 GnRH signaling pathway	2	1	3	BSA/Chit
ko04961 endocrine-regulated calcium reabsorption	1	2	3	Chit/PVP
ko04970 salivary secretion	2	1	3	BSA/Chit

through the mTOR signalling pathway[50] (Lunova *et al.* 2019, and references therein).

Discussion

In the current study, we provide more insight into molecular mechanistic responses underlying AgNP toxicity and the influence of particle size and coating type. Overall, we found a clear correlation with the number of regulated transcripts and Ag internal body concentrations, especially with regard to medium-sized AgNPs. This implies that total Ag elicits transcriptional alterations, but we are not able to distinguish between Ag ions and particulate Ag. This may indicate that the uptake of Ag from the AgNPs was ionic, as has been shown before.[21] Particle size and coating type clearly influenced the uptake kinetics of AgNPs, where medium-sized particles seemed to be optimal for uptake in *L. rubellus* under tested conditions.[51] Interestingly, the differentially regulated genes seem particle-specific when considering gene annotation information, both among differentially coated medium-sized particles and between $AgNO_3$ and AgNP exposures in general (Fig. 3). This suggests that besides Ag ions, particle size and coating type affected transcriptional responses in very specific ways. Coating- and size-specific induction of tumour necrosis factor (TNF)-α and reactive oxygen species was recently shown in a mouse macrophage cell line, suggesting activation of different molecular mechanisms[24] depending on particle size and coating type. Nevertheless, when generating more generic gene ontology and pathway-related information, commonalities emerged among the different exposure types. In general, ribosome metabolism seemed to be down-regulated, while several cell signalling pathways were up-regulated. Notably, oppositely charged particles affected these pathways in opposite ways. Finally, metallothionein (MT) was the only gene differentially regulated among all treatments. MT is a cysteine-rich peptide known to strongly bind free metal ions for chelation and detoxification, suggesting that detoxification of ionic Ag is a common feature in AgNP toxicity, regardless of size and coating type. Indeed, many studies using diverse model organisms[29,52,53] report on the activation of MT upon AgNP exposure, confirming the involvement of this gene in AgNP detoxification.

AgNP pre-exposure characterisation

Details of characterisation of the AgNPs used in this study had earlier been reported,[33] and therefore only briefly discussed here. The TEM images and UV-vis spectra from AgNP characterisation indicated that the primary particle sizes targeted by the synthesis were achieved. Also, the morphology of the particles was preserved after conjugation and lyophilisation processes for all coatings. The shapes of the SPR peaks in both MilliQ water and soil extract were generally preserved except for those of the 20 nm AgNP_PVP and 35 and 50 nm AgNP_Chit suspensions in soil extract, whose SPR peaks suggested formation of some agglomerates. The formation of agglomerates in the soil solution may explain the lower toxicity of these AgNPs, due to them becoming less bioavailable, as was similarly observed with C_{60} exposure.[54] Nevertheless, agglomeration may not necessarily imply the absence of adverse effects as the toxic potential of the AgNPs may change following ageing and decay, leading to the release of Ag as NPs or dissolved Ag^+ ions.[20,55–57] Depending on the surface coating used in our study, negative (AgNP_BSA), positive (AgNP_Chit) and "neutral" (AgNP_PVP) charges were obtained. Dispersion in soil extract also showed preserved ζ-potentials for AgNP_BSA and AgNP_Chit. All sizes of AgNP_PVP, however, presented negative ζ-potentials, but the values were less negative than those for AgNP_BSA.[33]

Ag uptake in earthworms

Total tissue concentrations showed that earthworms exposed to AgNPs or $AgNO_3$ accumulated Ag to varying degrees with mean values ranging from 15–80 mg Ag per kg tissue DW (Table 2). The uptake of AgNPs showed that the negatively charged AgNP_BSA was taken up the most, indicating some influence of the surface coating on the Ag uptake. There were no statistically significant differences in the uptake when comparing the three NP size ranges for each coating type.

 This journal is © The Royal Society of Chemistry 2020

Published on 19 February 2020. Downloaded by VRIJE UNIVERSITEIT on 3/1/2021 2:08:35 PM.

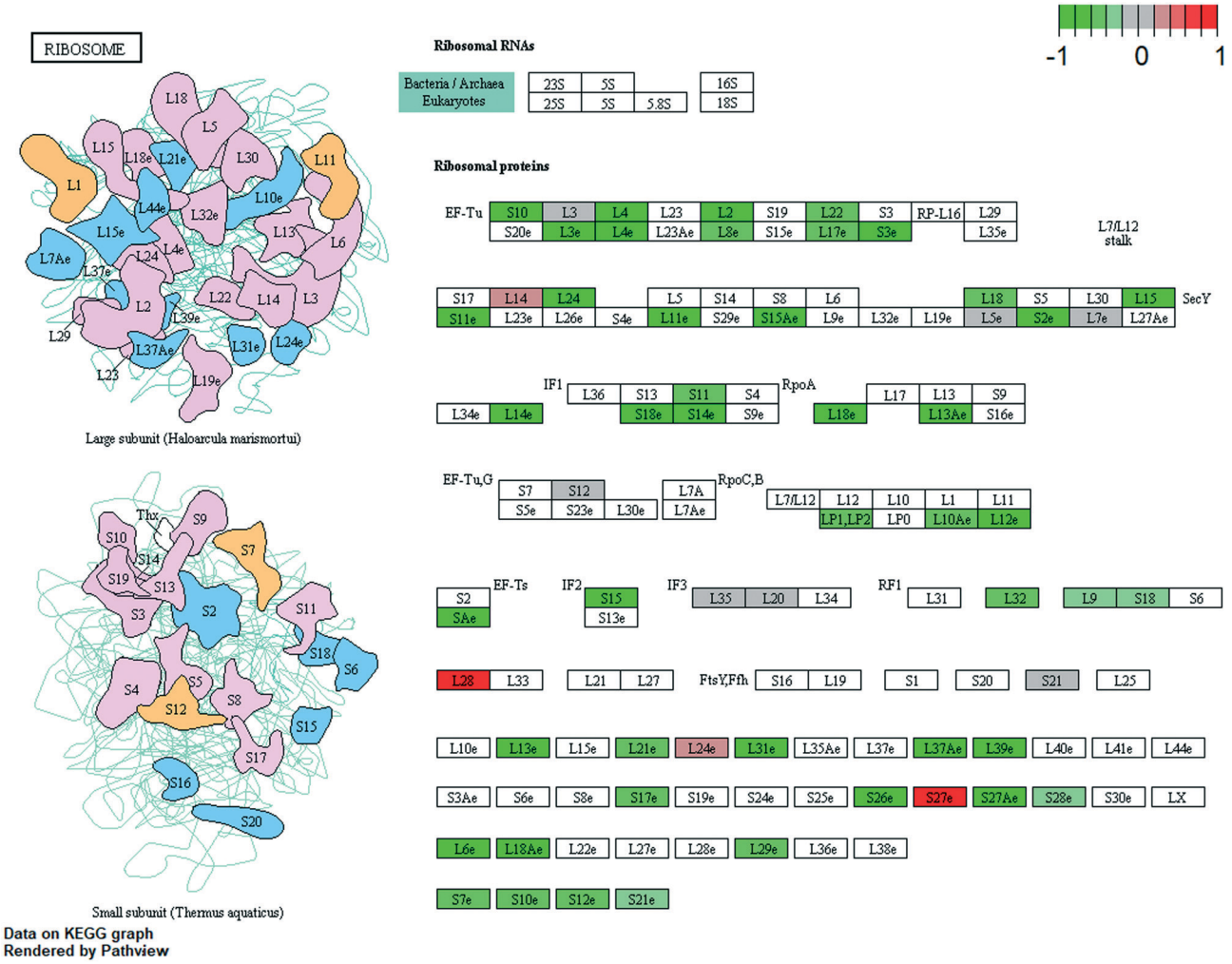

Fig. 4 Generally Applicable Gene-set Enrichment (GAGE) identifying significantly coordinated up- or down-regulation in biochemical pathways; results shown for KEGG pathway ko03010 ribosome with DEGs significantly regulated by 35 nm-sized AgNP_BSA exposure as input. Each box represents a protein coding gene involved in the assembly and function of the ribosome protein complex. Codes for protein identities are shown in each box and can be surveyed at https://www.genome.jp/dbget-bin/www_bget?ko03010. Classes of protein identities are shown by the following letters in the graph: S, small subunit ribosomal proteins; L, large subunit ribosomal proteins; 16S ribosomal RNA; 23S ribosomal RNA; 5S ribosomal RNA. Differential gene expression (fold change as compared to control levels) was color-coded and plotted on the KEGG derived pathway: red, up-regulation; green, down-regulation. This pathway is significantly coordinately down-regulated, as visualised by 46 protein-coding gene boxes that are colored green.

This suggests that for the different coating types, NP sizes did not have a significant effect on the outcome of exposures in the concentration range tested. Dissolution of the AgNPs was affected by the surface coating; the fact that the negatively charged AgNP_BSA caused most genes to be differentially expressed could partly be explained by the higher internal concentrations especially for the 35 nm sized particles (Fig. 2). The effects of the BSA coating on AgNP dissolution rates seem complex. Liu *et al.* showed that BSA enhances dissolution over short term exposures, while it provides protection against dissolution over extended times.[58] This suggests that BSA enhanced dissolution and most likely differential expression in our experiments, since we applied only a 72 hour exposure time. We speculate that the negative charge of AgNP_BSA even enhances this process in soil, since the soil matrix is negatively charged by itself, which keeps the AgNP_BSA particles in pore water solution. Why the medium-sized BSA coating exerts such pronounced effects remains unknown. Yet, AgNP_BSA previously showed the strongest effect on *in vivo* reproduction[33] as well as the highest *in vitro* induction of TNF-α in mammalian macrophage cells.[24] The uptake of Ag from $AgNO_3$ was in the same order of magnitude as that from the AgNPs when comparing nominal exposure concentrations on a mass basis (Table 2).

AgNP-induced differential transcription regulation

Comparing the DEGs responding to all medium-sized AgNP exposures to the DEGs responding to ionic Ag exposure, we

Published on 19 February 2020. Downloaded by VRIJE UNIVERSITEIT on 3/1/2021 2:08:35 PM.

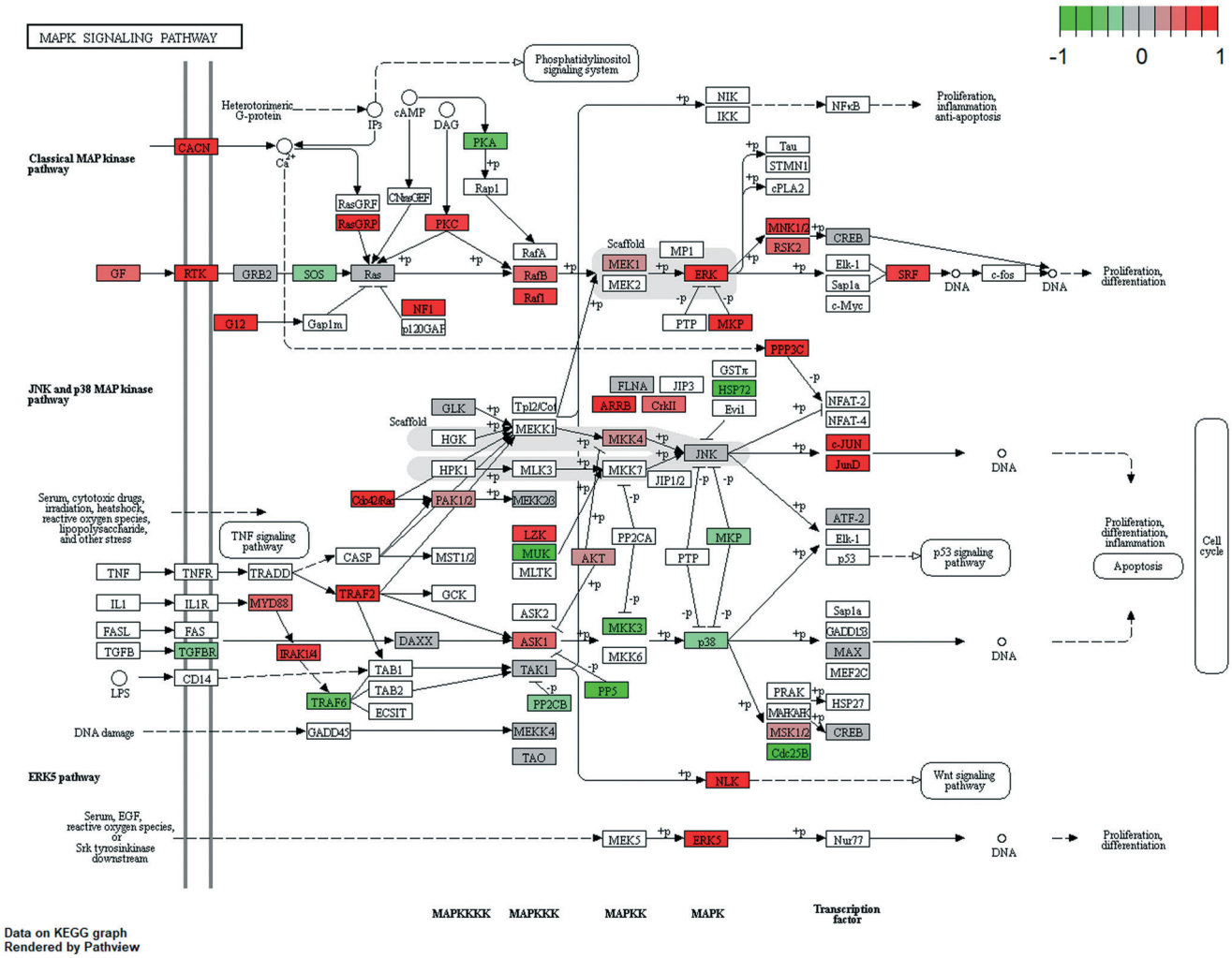

Fig. 5 Generally Applicable Gene-set Enrichment (GAGE) identifying significantly coordinated up- or down-regulation in biochemical pathways; results shown for KEGG pathway ko04010 MAPK signalling with DEGs significantly regulated by 35 nm-sized AgNP_BSA exposure as input. The mitogen-activated protein kinase (MAPK) cascade is a highly conserved module that is involved in various cellular functions, including cell proliferation, differentiation and migration. At least four distinctly regulated groups of MAPKs are expressed, extracellular signal-related kinases (ERK)-1/2, Jun amino-terminal kinases (JNK1/2/3), p38 proteins (p38alpha/beta/gamma/delta) and ERK5, that are activated by specific MAPKKs. Each box represents a protein-coding gene involved in MAPK signaling in animals. Codes for protein identities are depicted in each box and can be surveyed at https://www.genome.jp/dbget-bin/www_bget?ko04010. Differential gene expression (fold change as compared to control levels) were color-coded and plotted on the KEGG derived pathway: red, up-regulation; green, down regulation. This pathway is significantly coordinately up-regulated, as visualised by 32 protein-coding gene boxes that are colored red.

Table 4 Pathways that are significantly regulated ($p < 0.05$) in *Lumbricus rubellus* by all AgNP_BSA exposures in identical directions. ko numbers represent KEGG pathway codes

Pathways regulated by all AgNP_BSA exposures	
Up-regulated	Down-regulated
ko04014 Ras signaling pathway	ko03010 ribosome
ko04722 neurotrophin signaling pathway	ko04146 peroxisome
ko04012 ErbB signaling pathway	ko01212 fatty acid metabolism
ko04010 MAPK signaling pathway	ko01120 microbial metabolism in diverse environments
ko04510 focal adhesion	
ko04810 regulation of the actin cytoskeleton	

found 44% overlap. This confirms earlier observations of a transcriptome-wide study using *Eisenia fetida* exposed to AgNP_PVP[49] that some of the transcriptional responses caused by the AgNPs can be attributed to the release of Ag^+ ions from the core. This observation was further supported by the specific transcriptional profiles of the 37 genes responding to both nanoparticulate and ionic Ag. Besides MT, we identified the apoptosis-related cysteine peptidase caspase-7, which confirms previous evidence that AgNPs can induce apoptosis.[59,60] Also, pathogenic infection was reported to induce apoptosis in macrophages by modulating signaling that leads to TNF-α production,[61] but this could not be mechanistically confirmed in this study. Up-regulation of cystathionine beta synthase indicates that AgNPs as well as

 This journal is © The Royal Society of Chemistry 2020

Published on 19 February 2020. Downloaded by VRIJE UNIVERSITEIT on 3/1/2021 2:08:35 PM.

ionic Ag impact cysteine metabolism, a pathway that was elucidated to be significantly up-regulated in our GAGE analysis. We speculate that the demand for cysteine increases, due to increased biosynthesis of cysteine-rich MT to provide protection against free metal ions. It is also known that cysteine itself chelates with ionic Ag, which can even alleviate Ag toxicity in *E. coli*.[62] This suggests that ionic Ag can cause cysteine depletion through chelation, which could physiologically be counteracted by inducing cysteine biosynthesis.

Although the uptake of Ag may be in the ionic form following dissolution of AgNPs, either forms of Ag can be transformed into particulate Ag with Ag_2S and AgCl being the most common forms reported in the literature,[20] resulting in biogenically altered particulate Ag in earthworms.[21] Either or both particulate and ionic forms of Ag may determine the outcome of exposures, with transformation from particulate into ionic Ag or *vice versa*.[63–67] It was shown that after 28 days of exposure, >98% of the tissue Ag concentration of earthworms exposed to the same AgNPs as in the current study was in the form of ionic Ag^+.[33] This suggests that dissolution plays a significant role; however, it is not known how that affects the exposure after just 72 hours, which was the duration of the current study.

There was hardly any overlap when comparing the gene expression responses due to different sizes of AgNPs for each coating. This may likely be a result of the low numbers of DEGs responding to 20 and 50 nm sized AgNPs (Table 2). Internal accumulation of AgNP_BSA and AgNP_Chit in *L. rubellus* showed no significant difference associated with AgNP particle sizes.[33] In the case of AgNP_PVP accumulation, higher internal concentrations were observed for the smallest 20 nm particle size.[33] So, transcriptional regulation does not seem to be directly associated with Ag uptake, although most DEGs were associated with medium-sized AgNPs with relatively high accumulation. Also, no commonalities could be identified when comparing enriched biological processes and molecular functions, even among the medium sized particles (ESI† file 4). A similar result was found for the amphipod *Gammarus fossarum* exposed to AgNP_PVP or AgNP_Citrate. AgNP_PVP affected osmoregulation and cytoskeleton-related processes, while AgNP_Citrate seemed to affect DNA damage and repair through NF kappaB signaling.[68] Taken together, we can conclude that the molecular response to different NP surface coatings is highly context-dependent, which makes nanoparticle hazard assessment even more complex than we thought before.

When analyzing DEGs in the context of affected pathways, a more holistic picture starts to emerge. Notably, several important cell signaling pathways seemed severely affected. Nanoparticles, including AgNPs, are known to bind to cell surfaces, potentially impacting cytoskeletal organization and cell communication through signaling pathways.[69,70] As such, they influence cell morphology, mobility and communication,[70] which is also underpinned by the altered regulation of the actin cytoskeleton, focal adhesion pathway and Ras signaling pathway in this study. Moreover, research investigating the effects of AgNP exposure on cell lines provides evidence for MAPK signaling to be involved in actin filament dynamics and histone modification resulting in programmed cell death.[71–73] The components of focal adhesion, Ras signaling and MAPK signaling were all identified in association with AgNP toxicity in *L. rubellus* in this study and may provide a more generalized picture of the AgNP's mechanism of toxic action. Interestingly, focal adhesion, Ras signaling and MAPK signaling pathways were regulated in opposite ways when compared between AgNP_BSA (up-regulated signaling pathways) and AgNP_Chit (down-regulated signaling pathways). Since AgNP_BSA is negatively charged and AgNP_Chit is positively charged, we speculate that particle charge or released BSA and chitosan themselves may influence these signaling pathways in opposite directions. Further research is necessary to establish a causal link between particle charge, BSA or chitosan and modulation of cell signaling pathways.

Autophagy through mTOR signaling was very strongly up-regulated upon exposures to medium- and large-sized AgNP_BSA. Autophagy is a cellular degradation process, by which cytoplasmic material is transported to lysosomes for degradation. mTOR is a well-known key regulator of cell metabolic homeostasis, controlling proliferation, and programmed cell death, but is also a well-established negative regulator of autophagy.[74] Several studies already showed that NPs are internalized and subsequently trafficked into lysosomes.[75] The efficiency of this process is dependent on the corona of endogenous proteins that bind to the NP surface[76] and on the size of the NPs. In turn, differently coated NPs will attract different proteins on their surface, which affect the intracellular NP trafficking into lysosomes. Our current RNAseq data suggest that *L. rubellus* activated lysosomal trafficking upon AgNP_BSA exposure (supported by KEGG pathway analysis as well as GO enrichment analysis, see Fig. 5), while this was not the case for AgNP_Chit and AgNP_PVP exposures. Since BSA is suggested to enhance AgNP dissolution during short term exposure times,[58] this may result in higher uptake and higher amounts of biogenically produced particles in the tissues. This, in turn, could trigger the trafficking into the lysosomes. In any case, our results confirm the importance of coating type affecting differential internal biological processes.

AgNP toxicity had a strong negative effect on ribosome metabolism, except in the case of small- and large-sized AgNP_Chit exposures. Again, this confirms previous observations by Novo *et al.*,[49] showing strong regulation of ribosome-associated genes upon AgNP exposure in *Eisenia fetida*. Ribosomes are responsible for translation of mRNAs into proteins, and this process is inhibited upon AgNP exposure (Fig. 5). Eukaryotic cells respond to stress in general by phosphorylation of translation initiation factor 2, which will turn from a substrate of translation into an inhibitor of translation. This is a highly conserved mechanism in animals, also called integrated stress response, and shuts down bulk protein synthesis to redirect energy resources for

Published on 19 February 2020. Downloaded by VRIJE UNIVERSITEIT on 3/1/2021 2:08:35 PM.

stress adaptation and survival pathways.[77] Our previous study showed that the applied concentrations of AgNPs in this study indeed cause sublethal toxicity impacting reproductive output,[33] which at the molecular level may be explained by the general shut down of bulk protein synthesis.

Conclusion

Our study showed different levels of silver accumulation in tissues of earthworms during a 72 h AgNP exposure in soil, indicating early uptake of different AgNPs depending on particle size and coating type. Ag from AgNP_BSA accumulated more, and alterations in the gene expression profiles of earthworms reflected this, as the highest numbers of DEGs were encountered with exposures to these negatively charged AgNPs with the highest accumulation patterns. Surface coating (charge) therefore influenced the uptake and effects of the AgNPs in the earthworms. The 35 nm medium-sized AgNPs accumulated Ag to the highest extent and induced more DEGs than the 20 or 50 nm sized particles for all tested AgNPs, suggesting the likely role of size in accumulation and induction of effects. The majority of genes shared by both particulate and ionic Ag^+ treated earthworms were regulated in the same direction, and only one single gene (MT) was commonly expressed by earthworms from all treatment groups. Therefore, the role of Ag^+ ions in inducing gene expression effects following AgNP exposure was also indicated. Gene ontology enrichment as well as gene set enrichment for pathway analysis turned out to be highly instrumental to elucidate more general patterns of transcriptome-wide responses. AgNPs seem to affect several signalling pathways, some of which are involved in developmental processes. Finally, the ribosomal translation, responsible for protein synthesis in general, was down-regulated in most AgNP treatments. This is in line with several previous studies, suggesting that high cellular energy demanding protein synthesis is shut down under stressful conditions.[77,78] We also confirm previous conclusions drawn from an RNAseq study on AgNP exposure in *Eisenia fetida* suggesting that different uptake mechanisms and toxicokinetics exist for Ag^+ and AgNPs, where AgNPs interact specifically with cell surface components involved in endocytosis and cell signalling.[49]

Availability of data

Datasets generated during and/or analysed during the current study are available in the ESI.† *L. rubellus* transcriptome assembly including raw Illumina read data as well as Illumina RNA sequencing data is stored in NCBI's SRA and downloadable under Bioproject no. PRJNA566139. The assembly, including previous raw transcript data upon which it was built, is also available under Bioproject number PRJNA596978.

Funding

This work was financially supported by NanoNextNL, a micro- and nano-technology consortium of the Government of The Netherlands and 130 partners. Funding was also received from *Managing Risks of Nanoparticles*, MARINA (EU-FP7, contract CP-FP 263215) and the Strategic Research Fund entitled *Novel technologies* provided by the Ministry of Economic Affairs of The Netherlands. Synthesis and characterization of the AgNPs used in this study received support from the QualityNano Project (http://www.qualitynano.eu/) which is financed by the European Community Research Infrastructures under the FP7 Capacities Programme (Grant No. INFRA-2010-262 163).

Conflicts of interest

The authors declare no competing financial interest.

Acknowledgements

The authors gratefully acknowledge Prof. Peter Kille (University of Cardiff) for kindly providing the mapping references representing an assembled transcriptome previously generated.

References

1 M. E. Vance, T. Kuiken, E. P. Vejerano, S. P. McGinnis, M. F. Hochella, Jr., D. Rejeski and M. S. Hull, Nanotechnology in the real world: Redeveloping the nanomaterial consumer products inventory, *Beilstein J. Nanotechnol.*, 2015, **6**, 1769–1780.
2 R. Foldbjerg, X. Jiang, T. Miclăuş, C. Chen, H. Autrup and C. Beer, Silver nanoparticles – wolves in sheep's clothing?, *Toxicol. Res.*, 2015, **4**, 563–575.
3 I. R. L. TechNavio, *Global Silver Nanoparticles Market 2015–2019*, 2015, p. 60.
4 S. I. Gomes, A. M. Soares, J. J. Scott-Fordsmand and M. J. Amorim, Mechanisms of response to silver nanoparticles on Enchytraeus albidus (Oligochaeta): survival, reproduction and gene expression profile, *J. Hazard. Mater.*, 2013, **254–255**, 336–344.
5 F. Gottschalk, T. Sonderer, R. W. Scholz and B. Nowack, Modeled environmental concentrations of engineered nanomaterials (TiO(2), ZnO, Ag, CNT, Fullerenes) for different regions, *Environ. Sci. Technol.*, 2009, **43**, 9216–9222.
6 N. C. Mueller and B. Nowack, Exposure modeling of engineered nanoparticles in the environment, *Environ. Sci. Technol.*, 2008, **42**, 4447–4453.
7 K. Schlich, T. Klawonn, K. Terytze and K. Hund-Rinke, Hazard assessment of a silver nanoparticle in soil applied via sewage sludge, *Environ. Sci. Eur.*, 2013, **25**, 17.
8 Q. H. Tran, V. Q. Nguyen and A. T. Le, Silver nanoparticles: synthesis, properties, toxicology, applications and perspectives, *Adv. Nat. Sci.: Nanosci. Nanotechnol.*, 2013, **4**, 033001.
9 P. Rajanahalli, C. J. Stucke and Y. Hong, The effects of silver nanoparticles on mouse embryonic stem cell self-renewal and proliferation, *Toxicol. Rep.*, 2015, **2**, 758–764.
10 T. Yoisungnern, Y. J. Choi, J. W. Han, M. H. Kang, J. Das, S. Gurunathan, D. N. Kwon, S. G. Cho, C. Park, W. K. Chang, B. S. Chang, R. Parnpai and J. H. Kim, Internalization of silver nanoparticles into mouse spermatozoa results in poor

 This journal is © The Royal Society of Chemistry 2020

Published on 19 February 2020. Downloaded by VRIJE UNIVERSITEIT on 3/1/2021 2:08:35 PM.

fertilization and compromised embryo development, *Sci. Rep.*, 2015, **5**, 11170.

11 H. Xu, F. Qu, H. Xu, W. Lai, Y. Andrew Wang, Z. P. Aguilar and H. Wei, Role of reactive oxygen species in the antibacterial mechanism of silver nanoparticles on Escherichia coli O157:H7, *BioMetals*, 2012, **25**, 45–53.

12 D. K. Tiwari, T. Jin and J. Behari, Dose-dependent in-vivo toxicity assessment of silver nanoparticle in Wistar rats, *Toxicol. Mech. Methods*, 2011, **21**, 13–24.

13 S. I. Gomes, D. Hansen, J. J. Scott-Fordsmand and M. J. Amorim, Effects of silver nanoparticles to soil invertebrates: oxidative stress biomarkers in Eisenia fetida, *Environ. Pollut.*, 2015, **199**, 49–55.

14 C. Greulich, D. Braun, A. Peetsch, J. Diendorf, B. Siebers, M. Epple and M. Koller, The toxic effect of silver ions and silver nanoparticles towards bacteria and human cells occurs in the same concentration range, *RSC Adv.*, 2012, **2**, 6981–6987.

15 M. J. van der Ploeg, R. D. Handy, P. L. Waalewijn-Kool, J. H. van den Berg, Z. E. Herrera Rivera, J. Bovenschen, B. Molleman, J. M. Baveco, P. Tromp, R. J. Peters, G. F. Koopmans, I. M. Rietjens and N. W. van den Brink, Effects of silver nanoparticles (NM-300K) on Lumbricus rubellus earthworms and particle characterization in relevant test matrices including soil, *Environ. Toxicol. Chem.*, 2014, **33**, 743–752.

16 S. Makama, R. Peters, A. Undas and N. W. van den Brink, A novel method for the quantification, characterisation and speciation of silver nanoparticles in earthworms exposed in soil, *Environ. Chem.*, 2015, **12**, 643–651.

17 M. van der Zande, R. J. Vandebriel, E. Van Doren, E. Kramer, Z. Herrera Rivera, C. S. Serrano-Rojero, E. R. Gremmer, J. Mast, R. J. Peters, P. C. Hollman, P. J. Hendriksen, H. J. Marvin, A. A. Peijnenburg and H. Bouwmeester, Distribution, elimination, and toxicity of silver nanoparticles and silver ions in rats after 28-day oral exposure, *ACS Nano*, 2012, **6**, 7427–7442.

18 R. Foldbjerg, E. S. Irving, Y. Hayashi, D. S. Sutherland, K. Thorsen, H. Autrup and C. Beer, Global gene expression profiling of human lung epithelial cells after exposure to nanosilver, *Toxicol. Sci.*, 2012, **130**, 145–157.

19 S. J. Yu, Y. G. Yin and J. F. Liu, Silver nanoparticles in the environment, *Environ. Sci.: Processes Impacts*, 2013, **15**, 78–92.

20 B. Reidy, A. Haase, A. Luch, K. A. Dawson and I. Lynch, Mechanisms of Silver Nanoparticle Release, Transformation and Toxicity: A Critical Review of Current Knowledge and Recommendations for Future Studies and Applications, *Materials*, 2013, **6**, 2295–2350.

21 M. Baccaro, A. K. Undas, J. de Vriendt, J. H. J. van den Berg, R. J. B. Peters and N. W. van den Brink, Ageing, dissolution and biogenic formation of nanoparticles: how do these factors affect the uptake kinetics of silver nanoparticles in earthworms?, *Environ. Sci.: Nano*, 2018, **5**, 1107–1116.

22 C. M. Powers, A. R. Badireddy, I. T. Ryde, F. J. Seidler and T. A. Slotkin, Silver nanoparticles compromise neurodevelopment in PC12 cells: critical contributions of silver ion, particle size, coating, and composition, *Environ. Health Perspect.*, 2011, **119**, 37–44.

23 A. K. Suresh, D. A. Pelletier, W. Wang, J. L. Morrell-Falvey, B. Gu and M. J. Doktycz, Cytotoxicity induced by engineered silver nanocrystallites is dependent on surface coatings and cell types, *Langmuir*, 2012, **28**, 2727–2735.

24 S. Makama, S. K. Kloet, J. Piella, H. van den Berg, N. C. A. de Ruijter, V. F. Puntes, I. M. C. M. Rietjens and N. W. van den Brink, Effects of Systematic Variation in Size and Surface Coating of Silver Nanoparticles on Their In Vitro Toxicity to Macrophage RAW 264.7 Cells, *Toxicol. Sci.*, 2018, **162**, 79–88.

25 F. Ribeiro, C. A. M. Van Gestel, M. D. Pavlaki, S. Azevedo, A. M. V. M. Soares and S. Loureiro, Bioaccumulation of silver in Daphnia magna: Waterborne and dietary exposure to nanoparticles and dissolved silver, *Sci. Total Environ.*, 2017, **574**, 1633–1639.

26 S. Zhao, L. Xi and B. Zhang, Union Exon Based Approach for RNA-Seq Gene Quantification: To Be or Not to Be?, *PLoS One*, 2015, **10**, e0141910.

27 K. O. Mutz, A. Heilkenbrinker, M. Lonne, J. G. Walter and F. Stahl, Transcriptome analysis using next-generation sequencing, *Curr. Opin. Biotechnol.*, 2013, **24**, 22–30.

28 H. C. Poynton, J. M. Lazorchak, C. A. Impellitteri, B. J. Blalock, K. Rogers, H. J. Allen, A. Loguinov, J. L. Heckman and S. Govindasmawy, Toxicogenomic responses of nanotoxicity in Daphnia magna exposed to silver nitrate and coated silver nanoparticles, *Environ. Sci. Technol.*, 2012, **46**, 6288–6296.

29 J. Y. Roh, S. J. Sim, J. Yi, K. Park, K. H. Chung, D. Y. Ryu and J. Choi, Ecotoxicity of silver nanoparticles on the soil nematode Caenorhabditis elegans using functional ecotoxicogenomics, *Environ. Sci. Technol.*, 2009, **43**, 3933–3940.

30 M. J. van der Ploeg, J. H. van den Berg, S. Bhattacharjee, L. H. de Haan, D. S. Ershov, R. G. Fokkink, H. Zuilhof, I. M. Rietjens and N. W. van den Brink, In vitro nanoparticle toxicity to rat alveolar cells and coelomocytes from the earthworm Lumbricus rubellus, *Nanotoxicology*, 2014, **8**, 28–37.

31 M. J. Van Der Ploeg, R. D. Handy, L. H. Heckmann, A. Van Der Hout and N. W. Van Den Brink, C60 exposure induced tissue damage and gene expression alterations in the earthworm Lumbricus rubellus, *Nanotoxicology*, 2013, **7**, 432–440.

32 M. Giulia, A. Calisi and T. Schettino, Earthworm Biomarkers as Tools for Soil Pollution Assessment, *Soil Health and Land Use Management*, 2012, pp. 305–332, DOI: 10.5772/28265.

33 S. Makama, J. Piella, A. Undas, W. J. Dimmers, R. Peters, V. F. Puntes and N. W. van den Brink, Properties of silver nanoparticles influencing their uptake in and toxicity to the earthworm Lumbricus rubellus following exposure in soil, *Environ. Pollut.*, 2016, **215**, 870–878.

34 N. G. Bastús, F. Merkoçi, J. Piella and V. Puntes, Synthesis of Highly Monodisperse Citrate-Stabilized Silver Nanoparticles of up to 200 nm: Kinetic Control and Catalytic Properties, *Chem. Mater.*, 2014, **26**, 2836–2846.

Published on 19 February 2020. Downloaded by VRIJE UNIVERSITEIT on 3/1/2021 2:08:35 PM.

35 M. J. van der Ploeg, J. M. Baveco, A. van der Hout, R. Bakker, I. M. Rietjens and N. W. van den Brink, Effects of C60 nanoparticle exposure on earthworms (Lumbricus rubellus) and implications for population dynamics, *Environ. Pollut.*, 2011, **159**, 198–203.

36 A. Calisi, A. Grimaldi, A. Leomanni, M. G. Lionetto, F. Dondero and T. Schettino, Multibiomarker response in the earthworm Eisenia fetida as tool for assessing multi-walled carbon nanotube ecotoxicity, *Ecotoxicology*, 2016, **25**, 677–687.

37 O. V. Tsyusko, S. S. Hardas, W. A. Shoults-Wilson, C. P. Starnes, G. Joice, D. A. Butterfield and J. M. Unrine, Short-term molecular-level effects of silver nanoparticle exposure on the earthworm, Eisenia fetida, *Environ. Pollut.*, 2012, **171**, 249–255.

38 S. K. Misra, A. Dybowska, D. Berhanu, S. N. Luoma and E. Valsami-Jones, The complexity of nanoparticle dissolution and its importance in nanotoxicological studies, *Sci. Total Environ.*, 2012, **438**, 225–232.

39 A. M. Bolger, M. Lohse and B. Usadel, Trimmomatic: a flexible trimmer for Illumina sequence data, *Bioinformatics*, 2014, **30**, 2114–2120.

40 B. Langmead and S. L. Salzberg, Fast gapped-read alignment with Bowtie 2, *Nat. Methods*, 2012, **9**, 357–359.

41 A. Roberts and L. Pachter, Streaming fragment assignment for real-time analysis of sequencing experiments, *Nat. Methods*, 2013, **10**, 71–73.

42 D. J. McCarthy, Y. Chen and G. K. Smyth, Differential expression analysis of multifactor RNA-Seq experiments with respect to biological variation, *Nucleic Acids Res.*, 2012, **40**, 4288–4297.

43 Y. Benjamini and Y. Hochberg, Controlling the False Discovery Rate - a Practical and Powerful Approach to Multiple Testing, *J. R. Stat. Soc. Series B Stat. Methodol.*, 1995, **57**, 289–300.

44 A. Alexa, J. Rahnenfuhrer and T. Lengauer, Improved scoring of functional groups from gene expression data by decorrelating GO graph structure, *Bioinformatics*, 2006, **22**, 1600–1607.

45 F. Supek, M. Bosnjak, N. Skunca and T. Smuc, REVIGO Summarizes and Visualizes Long Lists of Gene Ontology Terms, *PLoS One*, 2011, **6**, e21800.

46 C. Pesquita, D. Faria, A. O. Falcao, P. Lord and F. M. Couto, Semantic similarity in biomedical ontologies, *PLoS Comput. Biol.*, 2009, **5**, e1000443.

47 Y. Moriya, M. Itoh, S. Okuda, A. C. Yoshizawa and M. Kanehisa, KAAS: an automatic genome annotation and pathway reconstruction server, *Nucleic Acids Res.*, 2007, **35**, W182–W185.

48 W. J. Luo, M. S. Friedman, K. Shedden, K. D. Hankenson and P. J. Woolf, GAGE: generally applicable gene set enrichment for pathway analysis, *BMC Bioinf.*, 2009, **10**, 160.

49 M. Novo, E. Lahive, M. Diez-Ortiz, M. Matzke, A. J. Morgan, D. J. Spurgeon, C. Svendsen and P. Kille, Different routes, same pathways: Molecular mechanisms under silver ion and nanoparticle exposures in the soil sentinel Eisenia fetida, *Environ. Pollut.*, 2015, **205**, 385–393.

50 M. Lunova, B. Smolkova, A. Lynnyk, M. Uzhytchak, M. Jirsa, S. Kubinova, A. Dejneka and O. Lunov, Targeting the mTOR Signaling Pathway Utilizing Nanoparticles: A Critical Overview, *Cancers*, 2019, **11**, 82.

51 L. Shang, K. Nienhaus and G. U. Nienhaus, Engineered nanoparticles interacting with cells: size matters, *J. Nanobiotechnol.*, 2014, **12**, 5.

52 S. Ghojavand, F. Bagheri and H. M. Tanha, Integrative meta-analysis of publically available microarray datasets of several epithelial cell lines identifies biological processes affected by silver nanoparticles exposure, *Comp. Biochem. Physiol., Part C: Toxicol. Pharmacol.*, 2019, **216**, 67–74.

53 C. S. Patricia, G. V. Nerea, U. Erik, S. M. Elena, B. Eider, D. W. Dario and S. Manu, Responses to silver nanoparticles and silver nitrate in a battery of biomarkers measured in coelomocytes and in target tissues of Eisenia fetida earthworms, *Ecotoxicol. Environ. Saf.*, 2017, **141**, 57–63.

54 D. Y. Lyon, J. D. Fortner, C. M. Sayes, V. L. Colvin and J. B. Hughe, Bacterial cell association and antimicrobial activity of a C60 water suspension, *Environ. Toxicol. Chem.*, 2005, **24**, 2757–2762.

55 E. Izak-Nau, A. Huk, B. Reidy, H. Uggerud, M. Vadset, S. Eiden, M. Voetz, M. Himly, A. Duschl, M. Dusinska and I. Lynch, Impact of storage conditions and storage time on silver nanoparticles' physicochemical properties and implications for their biological effects, *RSC Adv.*, 2015, **5**, 84172–84185.

56 S. Kittler, C. Greulich, J. Diendorf, M. Koller and M. Epple, Toxicity of Silver Nanoparticles Increases during Storage Because of Slow Dissolution under Release of Silver Ions, *Chem. Mater.*, 2010, **22**, 4548–4554.

57 R. Sekine, G. Brunetti, E. Donner, M. Khaksar, K. Vasilev, A. K. Jamting, K. G. Scheckel, P. Kappen, H. Zhang and E. Lombi, Speciation and lability of Ag-, AgCl-, and Ag2S-nanoparticles in soil determined by X-ray absorption spectroscopy and diffusive gradients in thin films, *Environ. Sci. Technol.*, 2015, **49**, 897–905.

58 C. Liu, W. N. Leng and P. J. Vikesland, Controlled Evaluation of the Impacts of Surface Coatings on Silver Nanoparticle Dissolution Rates, *Environ. Sci. Technol.*, 2018, **52**, 2726–2734.

59 Y. B. Ma, C. J. Lu, M. Junaid, P. P. Jia, L. Yang, J. H. Zhang and D. S. Pei, Potential adverse outcome pathway (AOP) of silver nanoparticles mediated reproductive toxicity in zebrafish, *Chemosphere*, 2018, **207**, 320–328.

60 J. Tang, X. J. Lu, B. Chen, E. Q. Cai, W. L. Liu, J. X. Jiang, F. F. Chen, X. D. Shan and H. J. Zhang, Mechanisms of silver nanoparticles-induced cytotoxicity and apoptosis in rat tracheal epithelial cells, *J. Toxicol. Sci.*, 2019, **44**, 155–165.

61 W. W. Navarre and A. Zychlinsky, Pathogen-induced apoptosis of macrophages: a common end for different pathogenic strategies, *Cell. Microbiol.*, 2000, **2**, 265–273.

62 Z. Guo, G. Q. Chen, G. M. Zeng, Z. Z. Huang, A. W. Chen, L. Hu, J. J. Wang and L. B. Jiang, Cysteine-induced hormesis effect of silver nanoparticles, *Toxicol. Res.*, 2016, **5**, 1268–1272.

 This journal is © The Royal Society of Chemistry 2020

Published on 19 February 2020. Downloaded by VRIJE UNIVERSITEIT on 3/1/2021 2:08:35 PM.

63 J. Liu and R. H. Hurt, Ion release kinetics and particle persistence in aqueous nano-silver colloids, *Environ. Sci. Technol.*, 2010, **44**, 2169–2175.
64 E. Navarro, F. Piccapietra, B. Wagner, F. Marconi, R. Kaegi, N. Odzak, L. Sigg and R. Behra, Toxicity of silver nanoparticles to Chlamydomonas reinhardtii, *Environ. Sci. Technol.*, 2008, **42**, 8959–8964.
65 P. V. Asharani, Y. Lian Wu, Z. Gong and S. Valiyaveettil, Toxicity of silver nanoparticles in zebrafish models, *Nanotechnology*, 2008, **19**, 255102.
66 S. K. Mwilu, A. M. El Badawy, K. Bradham, C. Nelson, D. Thomas, K. G. Scheckel, T. Tolaymat, L. Ma and K. R. Rogers, Changes in silver nanoparticles exposed to human synthetic stomach fluid: effects of particle size and surface chemistry, *Sci. Total Environ.*, 2013, **447**, 90–98.
67 K. R. Rogers, K. Bradham, T. Tolaymat, D. J. Thomas, T. Hartmann, L. Ma and A. Williams, Alterations in physical state of silver nanoparticles exposed to synthetic human stomach fluid, *Sci. Total Environ.*, 2012, **420**, 334–339.
68 K. Mehennaoui, S. Cambier, T. Serchi, J. Ziebel, E. Lentzen, N. Valle, F. Guerold, J. S. Thomann, L. Giamberini and A. C. Gutleb, Do the pristine physico-chemical properties of silver and gold nanoparticles influence uptake and molecular effects on Gammarus fossarum (Crustacea Amphipoda)?, *Sci. Total Environ.*, 2018, **643**, 1200–1215.
69 J. T. Buchman, N. V. Hudson-Smith, K. M. Landy and C. L. Haynes, Understanding Nanoparticle Toxicity Mechanisms To Inform Redesign Strategies To Reduce Environmental Impact, *Acc. Chem. Res.*, 2019, **52**, 1632–1642.
70 D. Septiadi, F. Crippa, T. L. Moore, B. Rothen-Rutishauser and A. Petri-Fink, Nanoparticle-Cell Interaction: A Cell Mechanics Perspective, *Adv. Mater.*, 2018, **30**, 1704463.
71 X. X. Zhao, Y. Y. Rao, J. Liang, S. K. Lin, X. M. Wang, Z. L. Li and J. H. Huang, Silver Nanoparticle-Induced Phosphorylation of Histone H3 at Serine 10 Involves MAPK Pathways, *Biomolecules*, 2019, **9**, 78.
72 S. Chattopadhyay, S. K. Dash, S. Tripathy, P. Pramanik and S. Roy, Phosphonomethyl iminodiacetic acid-conjugated cobalt oxide nanoparticles liberate Co++ ion-induced stress associated activation of TNF-alpha/p38 MAPK/caspase 8-caspase 3 signaling in human leukemia cells, *J. Biol. Inorg. Chem.*, 2015, **20**, 123–141.
73 A. Rinna, Z. Magdolenova, A. Hudecova, M. Kruszewski, M. Refsnes and M. Dusinska, Effect of silver nanoparticles on mitogen-activated protein kinases activation: role of reactive oxygen species and implication in DNA damage, *Mutagenesis*, 2015, **30**, 59–66.
74 R. Zoncu, A. Efeyan and D. M. Sabatini, mTOR: from growth signal integration to cancer, diabetes and ageing, *Nat. Rev. Mol. Cell Biol.*, 2011, **12**, 21–35.
75 A. E. Nel, L. Madler, D. Velegol, T. Xia, E. M. V. Hoek, P. Somasundaran, F. Klaessig, V. Castranova and M. Thompson, Understanding biophysicochemical interactions at the nano-bio interface, *Nat. Mater.*, 2009, **8**, 543–557.
76 F. Bertoli, D. Garry, M. P. Monopoli, A. Salvati and K. A. Dawson, The Intracellular Destiny of the Protein Corona: A Study on its Cellular Internalization and Evolution, *ACS Nano*, 2016, **10**, 10471–10479.
77 Y. Gordiyenko, J. L. Llácer and V. Ramakrishnan, Structural basis for the inhibition of translation through eIF2α phosphorylation, *Nat. Commun.*, 2019, **10**, 2640.
78 R. Kaempfer, L. Ilan, S. Cohen-Chalamish, O. Turgeman, L. S. Namer and F. Osman, Control of mRNA Splicing by Intragenic RNA Activators of Stress Signaling: Potential Implications for Human Disease, *Front. Genet.*, 2019, **10**, 464.